Journal of Robotics and Control (JRC)
Volume 3, Issue 6, November 2022
ISSN: 2715-5072, DOI: 10.18196jrc.v3i6.16064

A Comparative Study Between Convolution and Optimal Backstepping Controller for Single Arm Pneumatic Artificial Muscles

Amna Suri Ahmed [1*], Saleem Khalefa Kadhim [2]
[1] Control and System Engineering Dept., University of Technology, Baghdad 10066, Iraq
E-mail: [1] cse.20.06.@grad.uotechnology.edu.iq, [2] Saleem.K.Kadhim@uotechnology.edu.iq
*Corresponding Author

***Abstract*— This study was based on the dynamic modeling and parameter characterization of the one-link robot arm driven by pneumatic artificial muscles. This work discusses an up-to-date control design based on the notion of a conventional and optimal backstepping controller for regulating a one-link robot arm with conflicting biceps and triceps positions supplied by pneumatic artificial muscles. The main problems found in systems that utilize pneumatic artificial muscle as actuators are primarily the large uncertainties, non-linearities, and time-varying features that severely impede movement performance in tracking control. In consideration of the uncertainty, high nonlinearity, and external disturbances that can exist during the motion. Lyapunov-based backstepping control technique was utilized to assure the stability of the system with improved dynamic performance. The bat algorithm optimization method is utilized in order to modify the variables used in the design of the controller to enhance the efficiency of the suggested controller. According to the conclusions, a quantitative comparison of the response in the PAM actuated the arm model in the current study and earlier investigations with the Backstepping controlled system revealed fair agreement with a variation of 37.5% from the optimal classical synergetic controller. In addition, computer simulations were utilized in order to compare the effectiveness of the proposed conventional controls and the optimal background. It has been proven that an optimal controller can control the uncertainties and maintain the controlled system's stability.**

Keywords—Pneumatic artificial muscle; Backstepping control; Bat algorithm.

I. INTRODUCTION

Pneumatic artificial muscles (PAMs) appear to hold a lot of promise in industrial applications for innovative robot and manipulator models[1]. PAMs are used in contemporary robotic systems because they typically provide high-speed action skills, an uncomplicated working mechanism, and safety operations. The power produced by PAM actuators doesn't rely just upon pressure yet in addition on the condition of expansion, which adds one more wellspring of the spring-like way of behaving [2]. Since multilayer structures are the central component of these actuators, these PAMs that mimic human muscle movement are lightweight. [3], [4]

Biomechanics, bio-advanced mechanics, mechanical technology, and counterfeit appendage substitution have all utilized PAM actuators. Further, the PAMs are noiseless gadgets, they can be utilized in emergency clinic medicines to clamor delicate patients [5]. Due to their powerful/volume proportions, PAMs don't need a stuff framework to help power when contrasted with engine actuators. PAMs are exceptional-lightweight natural responsiveness, excellent specific work, elasticity [6], and are valuable for the regular recurrence of biped motion because of their gracefulness [7], [8]

PAMs have numerous disadvantages that characterize them. The PAMs combative structure is one disadvantage that can be addressed as compared to other actuators. Another major issue is the failure to control PAMs due to their high time-varying, nonlinear, and uncertain parameter structure [9], [10]

This is a result of the mechanics of the system containing several uncertain, non-linear, and unknown factors that prevent the development of an effective actuator tracking controller [11]. Additionally, they are quite sensitive. The operational ranges of the PAM systems are severely restricted by parameters affecting the systems such as viscosity, temperature, and supply pressure [12], [13].

Due to the importance of the operation of PAMs and as they mimic real muscles, PAM is a useful device for implementing the humanoid [14]. The control of pneumatic muscles is difficult because the physical parameters are nonlinear and time-varying [15].

To address difficulties related to the control of mechanical systems driven by aerobic muscles, several researchers have put forward various control solutions. Where PAM-actuated devices employ the most recent control methodologies.

Lilly [16] recommended sliding-mode adaptive controller for planar pneumatic muscle-powered robot arm. The actual configurations of the nonlinear functions, including the system mechanical parameters, such as link weights, lengths, and inertias, are required by this adaptive controller. In addition, their wide operating range has been significantly restricted due to their extreme sensitivity to parameters affecting the operation of PAM systems, like the temperature, viscosity, and applied pressure.

Scaff et al. [17] proposed a McKibben PAM-actuated with the regular Proportional-Integral-Derivative (PID) controller, position control of a one-degree-of-freedom (1-DOF) system. The Simulated Optimization Algorithm (SOA) is used to modify the PID controller's parameters in the

enhancement of the PID-controlled system's dynamic performance. The idea that optimization is performed offline, with no online response or effort made to counteract parameter fluctuations is a typical control issue. On the opposite side, simply put, the suspended block displaced by PAMs provides the system powered by the PAM.

Choi et al. [12] A method for controlling PAM-powered robots has been introduced that would replace the proportional pressure regulator (PPR) with a control unit consisting of several micro encoders and pressure switches to address capacitance problems associated with PPR. new controller may be able to reduce capacity requirements, but at the sacrifice of accuracy, according to the results of the trial evaluation. The controller is only there to save storage and relies on an on-off mechanism while ignoring the unpredictability in the system parameters.

Enzevaee et al. [18] proposed Active Force Control (AFC) system based upon Fuzzy Logic (FL) controllers to track the control of a single-link robotic arm. This outcome from simulation and experimentation was used to evaluate the proposed control method's sustainability and reliability in calming the interruptions that it was subjected to. The primary conclusion that has been presented is that input-output gain has been used to mimic the robot arm's dynamics. Furthermore, the tracking controller's use of a PID controller was unable to offset the system parameter uncertainty.

Al-Jodah and Khames [19] described a 1st order and 2nd order sliding mode control (SMC) to track the angular displacement of a single-link robotic arm powered by two PAMs. The ability of the presented controllers for reducing chattering in associated control outputs as well as their robustness against uncertainties in the system variables have been investigated. However, mainly concentrated on finding a solution to the chattering problem commonly associated with SMC architecture.

Medrano-Cerda et al. [20] designed a bi-muscular pneumatic muscle activator system, adaptive controller. Adaptive pole-placement control has been used to construct the PAM system's control strategy. The suggested adaptive scheme has been based upon indirect control strategies, where mathematical model and system variables are estimated based on on-line input and output data collected using the suggested model architecture, although the controller can provide viable accuracy and result in a high ratio of power to weight.

Boudoua et al. [21] To control the PAM-operated robotic arms and decrease the chattering in the signal out of the control, an NN-based Twisting Sliding Mode Controller (TSMC) was introduced. This study utilized two methods two-layer Neural networks (NN) and on-line adaptive learning in order to simulate nonlinear and unidentified robot dynamics. The present work was unable to totally eradicate chattering in the output signal from the control, and using NN structures up to approximation may reduce a controller's performance except if the required quantity and kind of activation functions are applied.

Jahanabadi [22] studied the implementation of an integrated regulator for the trajectory tracking of a PAM-actuated 2-planar link manipulator based upon Active Force Control and FL (AFCFL). The FL, is controlled by an outer loop PID controller and is used to choose the optimal structure of the inertial matrix requested for the AFC mechanism for the robot arm. In addition, the principal tracking controller was a PID controller and a fixed gain has been used in order to simulate the dynamic model, which is significantly different from the original model.

Previous research has shown that, despite significant advancements in PAM's development and various control strategies, there is still considerable work to be completed. The earlier research employed FL, NN, control based on optimization, nonlinear control based on SMC, or hybrid nonlinear control, which are all examples of advanced control systems. However, these controllers could not solve all major issue such as the uncertainty, non-linearity, and the chattering that appear in the output signal of the system.

It is worth mentioning that the PAM-actuated manipulator's architecture varies between studies. In contrast to earlier research. the Backstepping Control (BSC) technique is used in this study to develop a controller for tracing and controlling of the PAM--actuated one-link robot arm movement. The BSC theory is based on state-space theories, that are used in the development and management of extremely complicated and interconnected nonlinear systems. The BSC method is based upon a control approach that is suitable for a specific class of non-linear systems.

To deal with all these paramount problems, an adaptive control strategy is suggested for controlling the PAM-actuated one-link robot arm, which can transact effectively with the impact generated by parametric uncertainties in actuating muscles

The dynamic performance of this controllable system is directly impacted by the BSC's design variables. The Bat Algorithm has been used in order to enhance the systems with uncertainties in actuation muscles of PAM modeling, reduction of the chattering, and modify those parameters because the trial-and-error approach for calculating those components is challenging, time-consuming, and does not produce the optimal dynamic stability response, it is necessary for improving the dynamic performance regulation and detection. Bats served as the inspiration for this echolocation algorithm, which was originally created by Yang [23].

This research aims to develop BSC to maintain and coordinate the tracking of desired motion while reducing chattering, non-linearity, and uncertainty, in the manipulator arm that is operated by PAM in the system to maintain the stability of the system.

This paper's contribution is to develop a control strategy based on BSC theory for tracing the motion of a single-link robot arm actuated by pneumatic artificial muscles while taking into account parameter uncertainties in the muscles. The suggested technique is tenacious and capable of preventing chattering while also compensating for the parametric uncertainties.

Using the bat algorithm with the proposed controller design parameters to make progress in implementation can be

considered another contribution that can also be computed since it has never been dealt with in the literature on these PAM systems.

This paper will contain the following sections in a sequence:

- The dynamics and control model contains the derivation of the mathematical model of one link arm actuated by PAMs with suggestion BSC.
- The optimization of the system using the bat algorithm.
- Results and discussion show the simulation results and discussion of the control system and model response.
- Finally, the Conclusion section concludes the paper.

The methodology of this paper is described in the block diagram that is shown in Fig. 1. and it shows the sequence of portraying the contents of this research.

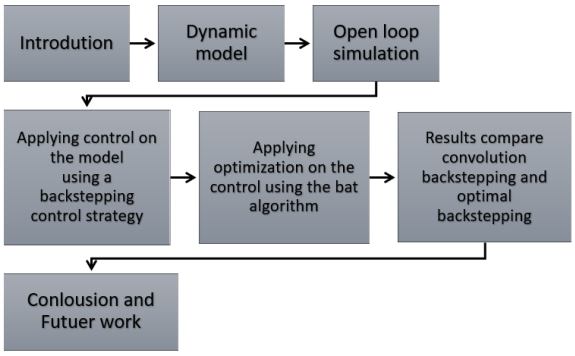

Fig. 1. Block diagram of the methodology.

II. DYNAMICS AND CONTROL MODEL

Fig. 1 shows a model of a PAM type and dimensions of the fluidic muscle that this study will concentrate on the fluidic muscle (DMSP-20-100N-RM-CM) from the FESTO Company. Because it responds more quickly than other types and movements like a natural muscle, its work efficiency is up to 50% closer to the biological muscles. Theoretical Fluidic Muscle force at maximum operating pressure is 1500N, the mode of operation is single-acting mode and pulling mode, and the maximum working load freely suspended is 80Kg. The operating pressure of this kind is between 0 MPa and 0.6 MPa [24].

Fig. 2 shows the two dimensions (2D) of the fluidic muscle type DMSP-20-100N-RM-CM. Also, the table1 illustrated the values of the dimensions.

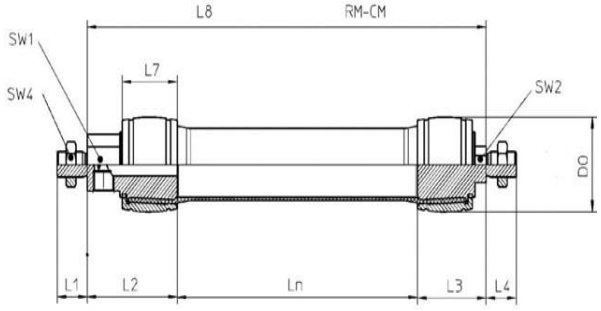

Fig. 2. Dimensions of the fluidic muscle type DMSP-20-100N-RM-CM [24]

TABLE I. DIMENSIONS VALUES [24]

Dimensions	value
SW1	17mm
SW2	10mm
SW4	13mm
L1	15mm
L2	36mm
L3	26mm
L4	15mm
L7	19mm
L8	142mm
LN	80mm
DO	22mm

Before starting the design control for the system utilizing PAM, it is required to 1st develop a mathematical model of the system that accurately reflects real muscle demeanor. The PAM system is able to be examined and its connected controller is designed to suit the implementation prerequisites.

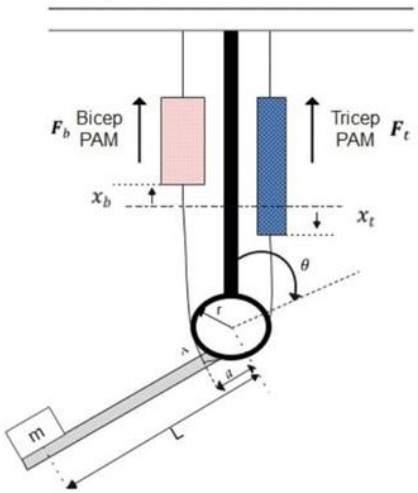

Fig. 3. PAM Single-Link Robot Arm

Fig. 3 shows a mass with PAMs actuated by arm positions of the triceps and biceps. The wrist moves as the PAMs expand and compress while the upper arm stays fixed. The upper arms and endpoints of the PMs are attached to a fixed reference point. where m denotes mass in (kg), g represents gravitational acceleration (m/s^2), r represents pulley radius (m), x_t represents pneumatic muscle extension (m), and x_b represents the muscle contraction (m). The PMs are attached to elbow at point A, which is a rotational axis away from the joint. L is distance between joint and the load's center of mass.

The extent to which pneumatic muscles extend x_t and muscles contract x_b can be represented respectively by Eq. (1) and (2) [16], [25]

$$x_b = a(1 - cos\,\theta) \quad (1)$$

$$x_t = a(1 + cos\,\theta) \quad (2)$$

The movement of the wrist shown an angle $\alpha = sin^{-1}(r/a)$ with the triceps corps. Within the same angle θ, the wrist is authorized to twist. The angle $\theta = 0$ corresponds to the wrist in a descending position, whereas angle $\theta = \pi$ represents a case that the wrist is positioned extremely

upwards. The wrist's biceps muscle produces a clock - wise torque that is provided by [26]:

$$\tau_{cw} = F_b(.)a\ sin\theta \tag{3}$$

in which the triceps muscle's counterclockwise torque is represented as:

$$\tau_{ccw} = F_t(.)r \tag{4}$$

where $F_t(.)$ and $F_b(.)$ represent developed forces from triceps and bicep of the PAMs, respectively, and r represents the radius of the pulley. The produced $F_t(.)$ and $F_b(.)$ may be described by the following dynamic PAM model [16], [25]:

$$F_b(.) = F(P_b) - K(P_b)x_b - B(P_b)x_b \tag{5}$$

$$F_b(.) = F(P_b) - K(P_b)x_b - B(P_b)x_b \tag{6}$$

Where bicep coefficients of viscous friction is $B(P_b)$, the L represents distance of the arms between the mass's centroid and joint, $B(P_t)$ represents triceps coefficients of viscous friction, $K(P_b)$ denotes bicep spring coefficients (N/m), $K(P_t)$ denotes triceps spring coefficients (N/m). $F(P_b)$ represents the force that is exerted by PAM in bicep case, $F(Pt)$ denotes force that has been exerted by PAM in triceps situations, a represents distance between joint axis of rotation and PAMs attached point (A), $F(P_b)$, $K(P_b)$ and $B(P_b)$ represent bicep PAM force, spring and viscosity coefficients, respectively, and those can be expressed in the following form:

$$\left.\begin{aligned} F(P_b) &= F_o + F_1P_b \\ K(P_b) &= K_o + K_1P_b \\ B(P_b) &= B_o + B_1P_b \end{aligned}\right\} \tag{7}$$

As well, $F(P_t)$, $K(P_t)$, and $B(P_t)$ characterizes triceps of the PAM force, spring, and viscosity coefficients, so that the associated formulas explain them:

$$\left.\begin{aligned} F(P_t) &= F_o + F_1P_t \\ K(P_t) &= K_o + K_1P_t \\ B(P_t) &= B_o + B_1P_t \end{aligned}\right\} \tag{8}$$

It is important to point out that coefficient B relying on whether a muscle is already in compressed mode or stretched mode, which is, one have varied coefficients of the triceps and bicep $B(P_t)$ and $B(P_b)$. Therefore, by combining the torques described by Eq. (3) and Eq. (4), one can find the dynamics motion equation:

$$I\ddot{\theta} = F_b(.)a\ sin\theta - F_t(.)r - MgL\ sin\theta \tag{9}$$

where $I = ML^2$ describes the moment of mass inertia about the elbow and latest term $(M * g * L * sin\theta)$ has been adjusted to take into consideration the mass gravity's counterclockwise torque on forearm. So can achieve the following by substituting Eq. (5) & Eq. (6) into Eq. (9):

$$\begin{aligned} &(F\ (P_b) - K\ (P_b)\ x_b - B_b\ (P_b)\ \dot{x}_b)\ a\ sin\ \theta - \\ &(F(P_t) - K(P_t)\ x_t - B_t(P_t)\ \dot{x}_t)\ r - MgL\ sin\ \theta \end{aligned} \tag{10}$$

It is provided time derivatives of PM extension x_t and contraction x_b may be described, respectively, as:

$$\dot{x}_b = a\ (sin\ \theta)\ \dot{\theta} \tag{11}$$

$$\dot{x}_t = -\ a\ (sin\ \theta)\ \dot{\theta} \tag{12}$$

Using Eq. (10) and (12), one can get

$$\begin{aligned} I\ddot{\theta} = {} & (F\ (P_b) - K\ (P_b)\ x_b - B_b\ (P_b)\ \dot{x}_b)\ a\ sin\ \theta \\ & - (F(P_t) - K(P_t)\ x_t \\ & - B_t(P_t)\ \dot{x}_t)\ r - M\ g\ L\ sin\ \theta \end{aligned} \tag{13}$$

The following is the triceps and biceps PAM pressure:

$$P_b = P_{ob} + \Delta P \tag{14}$$

$$P_t = P_{ot} - \Delta P \tag{15}$$

where P_{0t}, P_{0b} represent primary pressure of triceps and biceps, respectively, ΔP is designated as system's control input, and it displays how much pressure exists between both the triceps and biceps. Then combined the Eq. (14) and (16), to produce:

$$\begin{aligned} I\ddot{\theta} = {} & [(a\ F_0 + a\ F_1\ P_{0b} - M\ g\ L)\ sin\ \theta \\ & + a^2(\ K_0 + \ K_1\ P_{0b})\ sin\ \theta\ (cos\ \theta \\ & - 1) \\ & - a^2\ (B_{0b} + B_{1b}P_{0b})\ sin^2\theta.\dot{\theta} \\ & + a\ r\ (K_0 + K_1P_{0t})\ (1 + cos\ \theta) \\ & - a\ r\ (B_{0t} + B_{1t}P_{0t})\ sin\ \theta\ .\dot{\theta} \\ & - r\ (F_0 + F_1P_{0t})] + [a\ F_1\ sin\ \theta \\ & + a^2\ K_1\ sin\ \theta\ (cos\ \theta - 1) \\ & - a^2\ B_{1b}\ sin^2\theta.\dot{\theta} \\ & - a\ \ r\ K_1\big(1 + cos\ \theta\big) \\ & + a\ r\ B_{1t}\ \ sin\ \theta\ .\dot{\theta} + r\ F_1\big]\Delta P \end{aligned} \tag{16}$$

Eq. (16) could be expressed more succinctly as follows:

$$\ddot{\theta} = f\big(\theta, \dot{\theta}\big) + b\big(\theta, \dot{\theta}\big)\Delta P \tag{17}$$

Where is $f\big(\theta, \dot{\theta}\big)$ and $b\big(\theta, \dot{\theta}\big)$ are described by

$$f\big(\theta, \dot{\theta}\big) = \sum_{1}^{6} f_i Z_i\ \big(\theta, \dot{\theta}\big) \tag{18}$$

$$b\big(\theta, \dot{\theta}\big) = \sum_{1}^{6} b_i\ Z_i\ \big(\theta, \dot{\theta}\big) \tag{19}$$

where $i = 1, 2, \dots, 6$. The classification of coefficients' factors f_i, Z_i and b_i have been listed in Table 2. The difference between the pressures is the ΔP and given in Eq. (14) is characterized as a control signal; that is $u = \Delta P$. additionally, if state variable x_1 is assigned to angular position θ and state variable x_2 denotes angular velocity θ, then the following describes a state space representation: Eq. (20) [27]:

$$\begin{aligned} x_1 &= \theta, \\ \dot{x}_1 &= \dot{\theta} = x_2 \\ \dot{x}_2 &= \ddot{\theta} = \ddot{x}_1 = f\big(\theta, \dot{\theta}\big) + b\big(\theta, \dot{\theta}\big) \\ u &= f\ (x_1, x_2) + b\ (x_1, x_2)u \end{aligned} \tag{20}$$

Fig. 4 presents the MATLAB/SIMULINK /R2019a for the PAM actuated arm. The simulation of PAM actuated arm; the model representation is by using Equation (20). Table 3 displays the values of the PAM model's actuated arm variables that were used in the simulations.

TABLE II. CLASSIFICATIONS OF THE COEFFICIENT FACTORS f_i, Z_i AND b_i [25]

Z_i	f_i	b_i
$z_1 = \sin x_1$	$f_1 = (a F_0 + a F_1 P_{0b} - M g L) / I$	$b_1 = aF_1/I$
$z_2 = \sin x_1 (\cos x_1 - 1)$	$f_2 = a^2(ko + K_1 P_{ob})/I$	$b_2 = a^2 K_1/I$
$z_3 = (\sin^2 x_1)x_2$	$f_3 = -a^2 (B_{0b} + B_{1b} P_{ob})/I$	$b_3 = -a^2 B_{1b}/I$
$z_4 = 1 + \cos x_1$	$f_4 = a r (ko + K_1 P_{0t})/I$	$b_4 = -a r K_1/I$
$z_5 = (\sin x_1)x_2$	$f_5 = -a r (B_{0t} + B_{1t} P_{0t})/I$	$b_4 = -arK_1/I$
$z_6 = 1$	$f_6 = (-r F_0 - r F_1 P_{0t})/I$	$b_6 = rF_1/I$

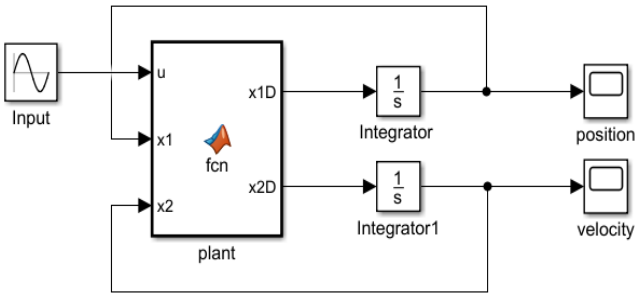

Fig. 4. Open loop PAM manipulator arm system represented by MATLAB SIMULINK.

The system as well as controller have both been modelled using the MATLAB/SIMULINK software suite. The outputs of the open loop position and velocity are shown in Fig. 5. The PAM's motion is the main issue since it is unstable and unmanageable due to the lack of speed control, which in turn results in undesirable movement that needs to be regulated. Fig. 5. shows that the open loop system is unstable. In order to stabilize the PAM and move its states to the equilibrium point area, the Backstepping controller is used.

Table 3 lists the mathematical values for both PAM-actuated Single Arm Manipulators in the bicep/triceps positions

TABLE III. NUMERICAL SYSTEM PARAMETER VALUES [25]

Coefficient Descriptions	Values
The nominal force that has been exerted by PAM (F_0)	0.986×10^2 N
Variation in a force exerted by PAM (F_1)	$0.803N$
Bicep /variation in viscosity coefficient (B_{1b})	4.66×10^{-3}N. s /m
Bicep /nominal viscosity coefficient (B_{0b})	1.35N. s/m
Nominal spring coefficient (k_0)	6.51N/m
Triceps /nominal viscosity coefficient (B_{0t})	4.03×10^{-1}N. s /m
Triceps /variation in viscosity coefficient (B_{1t})	12.0×10^{-4}N. s /m
Nominal bicep pressure (P_{ob})	510.4KPa
Variation in spring coefficient (k_1)	2.12×10^{-2}N/m
The distance from the mass center to the joint (L)	0.46m
Nominal triceps pressure (P_{ot})	400Pa
Mass (M)	20g
Pulley radius (r)	0.0508m
Distance from PAM attached point to the joint axis (a)	0.0762m
Gravity Acceleration (g)	9.8m/s^2

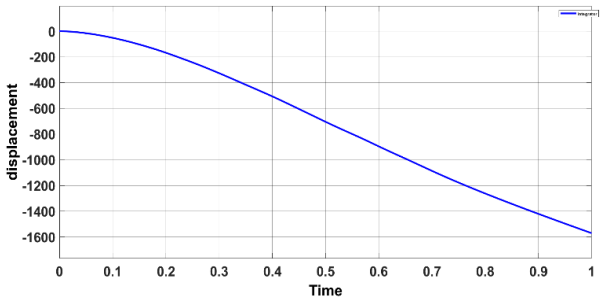

Position of the single-arm robot

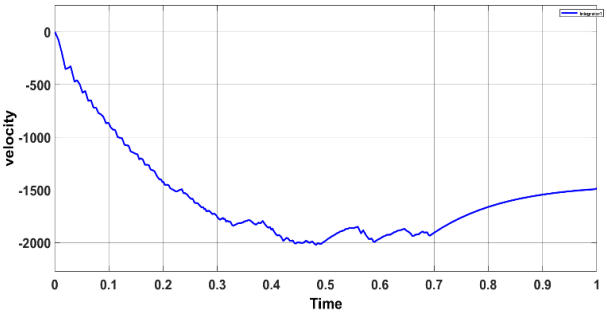

Velocity of the single-arm robot

Fig. 5. Open-loop response of Single Arm PAM-Actuated Robot.

III. BACKSTEPPING CONTROL DESIGN (BSC)

The control methods for analyzing the control design for the movement of the PAM robot arm have been developed in this section. A BSC approach is used to develop the control design [28][29]. The backstepping controller's design variables directly affect how dynamically responsive the controlled system is [30]. Follow the steps mentioned to establish the BSC algorithm for a Single Arm PAM-Actuated Robot system [31].

Let the variation between actual angle position $x_1 = \theta$ and needed trajectory $x_{1d} = \theta_d$ be the e as the follow [30], [32][33] is:

$$e_1 = x_1 - x_{1d} \tag{21}$$

The error's time derivative, can be written as follows in Eq. (21):

$$\dot{e_1} = \dot{x}_1 - \dot{x}_{1d} \tag{22}$$

Defining the first virtual control $\alpha_1 = x_2$ and sub in Eq. (22) to get:

$$\dot{e_1} = \alpha_1 - \dot{x}_{1d} \tag{23}$$

The Lyapunov function is a positive function and the function derivative [34]:

$$V_1 = \frac{1}{2} e_1^2 \tag{24}$$

$$\dot{V}_1 = e_1 \dot{e}_1 \tag{25}$$

as following, going to substitute Eq. (23) in the Eq. (25) to get the function of Lyapunov, which can be written as follows:

$$\dot{V}_1 = e_1(\alpha_1 - \dot{x}_{1d}) \tag{26}$$

A virtual control ($\alpha_1 = -c_1 e_1 + \dot{x}_{1d}$) is generated and sub into Eq. (26) then:

$$\dot{V}_1 = -c_1 e^2{}_1 \quad (27)$$

This implies $V_1 < 0$ Let the error e_2, between actual state $x_2$and the first virtual control α_1 described by taking time derivative of Eq. (28) and utilizing Eq. (20) to get:

$$e_2 = x_2 - \alpha_1 \quad (28)$$

$$\dot{e_2} = \dot{x_2} - \dot{\alpha_1} \quad (29)$$

$$\dot{e_2} = f(x_1, x_2) + b(x_1, x_2)u - \dot{\alpha_1} \quad (30)$$

The second Lyapunov function is:

$$V_2 = \frac{1}{2} e_1^2 + \frac{1}{2} e_2^2 \quad (31)$$

Utilizing time derivative of Lyapunov function

$$\dot{V}_2 = e_1 \dot{e_1} + e_2 \dot{e_2} \quad (32)$$

$$\dot{V}_2 = -c_1 e^2{}_1 + e_2 (f(x_1, x_2) + b(x_1, x_2)u - \dot{\alpha_1}) \quad (33)$$

Choosing the control law:

$$u = \frac{-c_2 e_2 + e_1 + f(x_1, x_2) + c_1 \dot{e_1} - \ddot{x}_{1d}}{b(x_1, x_2)} \quad (34)$$

The result of the Lyapunov function's derivative is:

$$\dot{V}_2 = -c_1 e^2{}_1 - c_2 e^2{}_2 \quad (35)$$

where, c_1 and c_2 represent positive constant that is to be determined with the use of the Bat algorithm and $V_2 < 0$ are negative definite [35][36].

Fig. 6 display graphical design of backstepping control for PAM - actuated robot arm and shows the control law that controls t he PAM-actuated robot arm

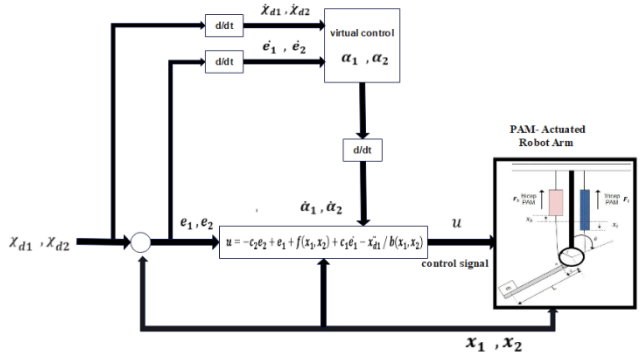

Fig. 6. Schematic diagram of the proposed BSC for PAM.

A. Optimal Backstepping Control Parameters

All control systems must operate accurately in both steady-state and transient conditions with a low error rate. there are plenty of methods to optimize the results and improve the control to get better outcomes such as particle swarm optimization (PSO) [37], chaotic particle swarm optimization (CPSO) [38], cuckoo search optimization (CSO) [39], modified chaotic invasive weed optimization (MCIWO) [40]and bat algorithm [41]. In this paper using bat algorithm to optimize the model control. The output and stability of the system are affected by the backstepping algorithm's parameters The objective of the present study is to select the optimal parameters control value for the PAM-Actuated robot arm. These two design parameters are referred to as c_1 and c_2. BAT is modeled after how common bats use active sonar to determine where to find food [42]. The Bat method is a popular met heuristic algorithm for resolving practical optimization issues. The Bat must be used by three principles: To begin started, all bats utilize the echolocation in order to measure their distance from a given spot. Second, bats fly in a predetermined direction at a predetermined speed at irregular intervals with a fixed frequency [43]. The volume and wavelength, however, can change. As a result, Bats immediately change their wave-lengths to match their target. Thirdly, the authors believed that the best approach to varying volume is to go from the loudest to the quietest [23]. Different algorithms can be developed inspired by bats, or called bat algorithms. For simplicity, now Using the following rough or idealistic guidelines:

1) All the bats utilize echolocation to determine the range and somehow magically distinguish between background obstacles and food/prey
2) In order to find prey, bats fly at random with a velocity of v_i, a position of x_i, a fixed frequency of f_{min} , a variable wave-length, and a loudness of A_0. Depending on how close their target is, they can automatically modify pulses' wave-length (or frequency) and rate of emission (element $r \in [0, 1]$).
3) Despite the fact that there are numerous ways in which the loudness can change, we suppose that it changed from a high (positive) A_o to a minimal constant value A_{min} [44].

Additionally, to the previous principles, frequencies and wavelengths are typically set so that they closely reflect the size of the zone of interest. In practical applications, frequency and wavelengths occur within the ranges of $[f_{min}, f_{max}]$ and $[\lambda_{min}, \lambda_{max}]$ correspondingly. It is necessary to develop procedures to ascertain the positions and velocities of the virtual bats in d-dimensional study space in order to solve an optimization model using them. The new position X_i^t it and velocity V_i^t it are defined as follows at time step t:

$$f_i = f_{min} + (f_{max} - f_{min}) \quad (35)$$

$$V_i^t = V_i^{t-1} + (X_i^t - X_*) f_i \quad (36)$$

$$X_i^t = X_i^{t-1} + V_i^t \quad (37)$$

here, the $\beta \in [0-1]$ represents random vector that has been taken from uniformly distributed; $X *$ represents current global best location (i.e., solution) as determined through the comparison of all of the solutions for all of the n bats.

A new solution is represented locally for each bat using random walk once a solution has been selected from among actually better possibilities for local research.

$$X_{new} = X_{old} + \in A^t \quad (39)$$

In the case where the bat locates a prey, the level of the sound drops and the pulse emission rate rises. The bat is heading to optimum solution based on:

$$A_i^{t+1} = \alpha A_i^t, r_i^{t+1} = r_i^{\circ}[1 - e_i^{-yt}] \quad (40)$$

here, α and γ are constants ($\alpha = \gamma = 0.90$), the initial emission rate is $r^o \in [0 - 1]$, and initial loudness is $A_i \in [0.1 - 0.9]$.

The $[c_1, c_2]$ variables of the suggested controller for a PAM-Actuated robot arm are tuned using BAT methods. The BSC determines and sets the optimized design variable at the algorithm's conclusion. The BA has set the size of the population at 40 and the maximum number of iterations at 100. Mean Square Error (MSE), which may be calculated as follows, is chosen as the cost function which will be utilized in order to assess every one of the particles during the search for minimum.

$$MSE = \frac{1}{n}\sum_{t=1}^{n} e_1(i)^2 \quad (41)$$

where, $e_1 = x_1 - x_{1d}$, n represents sampling number [45].

Fig. 7 shows cost function's behavior as algorithm iteration function. at the number of iterations of, 40 the cost stabilized.

TABLE IV. OPTIMUM AND TRIAL-AND-ERROR VALUES OF CONTROLLER DESIGN PARAMETERS

parameters	Values
c_1	83.3419
c_2	121.4274

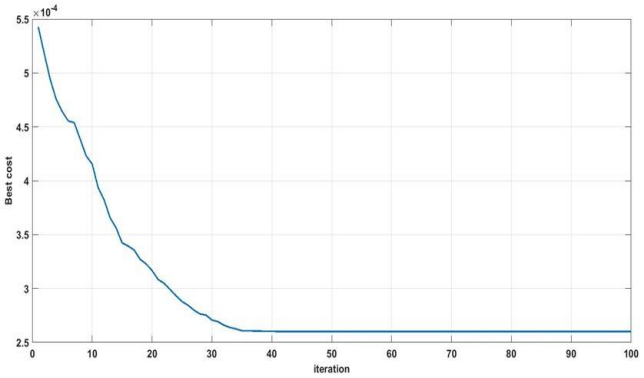

Fig. 7. Cost function's behavior as algorithm iteration function.

Finally, the BSC sets those optimum values so as to achieve a system that is controlled by the optimal BSC.

V. SIMULATION RESULTS AND DISCUSSION

In this section describes a BSC designed for single-arm PAM-actuated robot stabilization, tracking, and regulatory control. Using MATLAB/SIMULINK/2019a simulation to analyze the performance of the BSC and evaluate the controller. The coefficient values affecting the system for a single-arm PAM-actuated robot are displayed in Table 3. Backstepping controllers based on the try-and-error approach and the Bat algorithm have been compared in terms of performance using the MSE as a performance measure. Table 5. includes the controller design parameter's optimal and trial-and-error values.

The current BSC algorithm was validated against Humaidi et al. [46] A comparison was accomplished using the response of stability the position tracking for the PAM actuated arm moving. As mentioned previously that the BSC algorithm requires validation as well. The BSC scenario investigates the response of stability the position tracking when using the proposed BSC with bat algorithms scheme and optimal classical synergetic controller (CSC). The comparison has been performed with the use of the position tracking in the valve during PAM actuated arm moving. The time response for PAM actuated arm moving was obtained from the optimal classical synergetic controller (CSC) reaching its stable state at 4sec, whereas response as a result of the non-optimal CSC reaches the equilibrium at stable state at 6.5sec. but response of using the optimal BSC reaches its steady at 2.5 sec, while non-optimal reaches its steady-state at 6 sec. Backstepping controllers based on the try-and-error method and the Bat algorithm have been compared in terms of performance using the MSE as a performance measure.

TABLE V. OPTIMAL DESIGN PARAMETER VALUES

Parameter	Optimal values	Assuming values
c_1	83.3419	1
c_2	121.4274	1

Primary parameters determining performance of the PAM actuated arm include arm position and velocity. A series of the isolated time steps at different PAM actuated arm movements are shown in Figs. 8, 9, 10, 11, and 12 to present the performance of the PAM actuated arm under investigation.

Fig. 8 shows the position's control signal using the BSC technique, the control signal tracking shows that at time 6 sec reaches its steady-state but the signal has chattering and not smooth. The error between the desired signal and the position with non-optimal BSC is 4×10^{-5}.

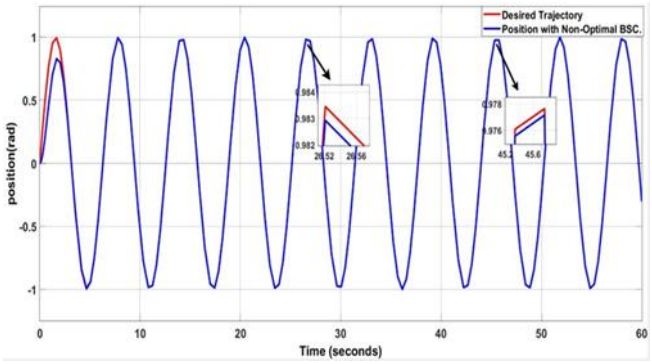

Fig. 8. Position trajectory for BSC.

Fig. 9 shows the control signal for the position by applying the BAT algorithm with BSC. According to the figure, the system exhibits excellent convergence and high levels of stability in a limited time the signal reaches its steady-state at 0.5 sec and the chattering is smaller, and the signal is smoother. The error between the desired signal and optimal BSC position signal is 1.376×10^{-6}.

The position tracking results show how much better the proposed BSC with Bat algorithms method is than the BSC at tracking positions. Furthermore, the use of Bat algorithms minimized the tracking position error and the chattering that happened with the BSC tracking position signal.

Fig. 10 shows how the comparison between the optimal BSC, convolution BSC, and the desired trajectory.

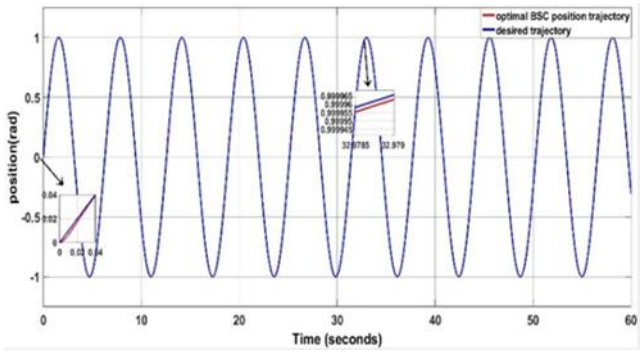

Fig. 9. Position trajectory for optimal with BSC.

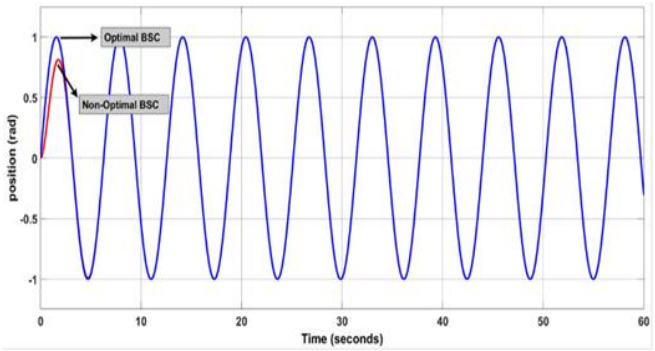

(a)

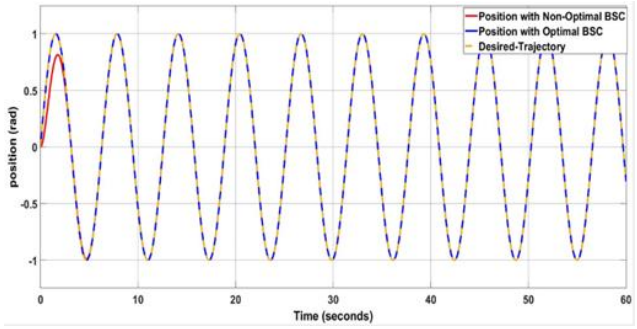

(b)

Fig. 10. Compare signals (a) compare between optimal and Convolution Backstepping control (b) compare optimal, Convolution, and desired trajectory signals.

Figs. 8 and 9 shows how much smoother the position tracking is when using the proposed BSC with bat algorithms scheme than when using the Backstepping control. Additionally, the tracking position error was reduced significantly using bat algorithms.

The BSC maximum tracking error for the position tracking trajectory is 0.4 percent at peak. Therefore, a careful analysis of the data reveals that the ideal BSC method reduces tracking errors for the position by a factor of 0.004%. Additionally, the velocity tracking errors presented in Fig. 10. show how much the tracking performance is improved by employing BSC in combination with bat algorithms. Figs. 11 (a-b) show that bat algorithms have an increased tracking velocity for the desired trajectory.

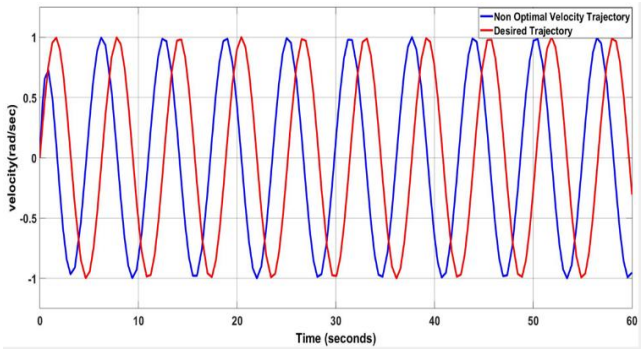

(a)

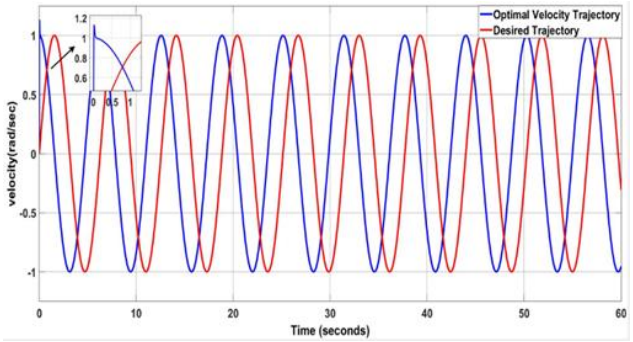

(b)

Fig. 11. Velocity trajectory (a)Velocity trajectory with convolution BSC, (b) the Velocity trajectory with optimal BSC.

VI. CONCLUSION

The PAM actuated arm was designed and developed in this research utilizing the Backstepping method, It involves modifying the system's equations to incorporate a new state. It is shown that the control law is in charge of providing precise monitoring of the required trajectory for the movements of the arm manipulator. By simulating the control scheme using MATLAB/2019/b. The Bat method is employed to determine the best design parameters for improved dynamic performance, which eliminates the requirement for a trial-and-error method of fine-tuning the design BSC. The accuracy of the simulation results was confirmed by comparing them to those published in previous works on Adaptive Synergetic Control Design. The comparison revealed that utilizing BSC reduces error and employing optimal BSC increases accuracy. As compared to backstepping control using try-and-error parameters the error is 0.4% however, according to the proposed BSC with BA conclusions, the PAM actuated arm has a position inaccuracy of 0.004%.

The future work in this research will focus on a comparative study that can be achieved by utilizing an adaptive control strategy for the same control, robot configuration, the same conditions and same parameters, in addition to benefiting from the improvement of the bat method on the proposed adaptive control and comparing the results.

REFERENCES

[1] Z. Situm and S. Herceg, "Design and control of a manipulator arm driven by pneumatic muscle actuators," in *2008 16th Mediterranean Conference on Control and Automation*, pp. 926–931, Jun. 2008, doi: 10.1109/MED.2008.4602136.

[2] N. Z. Azlan and N. Kamarudzaman, "Soft Pneumatic Exoskeleton for Wrist and Thumb Rehabilitation," *International Journal of Robotics and Control Systems*, vol. 1, no. 4, pp. 440–452, 2021, doi: https://doi.org/10.31763/ijrcs.v1i4.447.

[3] D. B. Reynolds, D. W. Repperger, C. A. Phillips, and G. Bandry, "Modeling the Dynamic Characteristics of Pneumatic Muscle," *Ann Biomed Eng*, vol. 31, no. 3, pp. 310–317, Mar. 2003, doi: 10.1114/1.1554921.

[4] D. W. Repperger, K. R. Johnson, and C. A. Phillips, "A VSC position tracking system involving a large scale pneumatic muscle actuator," in *Proceedings of the 37th IEEE Conference on Decision and Control (Cat. No.98CH36171)*, 1998, vol. 4, pp. 4302–4307, doi: 10.1109/CDC.1998.761982.

[5] A. J. Humaidi, S. K. Kadhim, M. E. Sadiq, S. J. Abbas, A. Q. Al-Dujaili, and A. R. Ajel, "Design of optimal sliding mode control of pam-actuated hanging mass," *ICIC Express Letters*, vol. 16, no. 11, 2022.

[6] R. M. Robinson, C. S. Kothera, and N. M. Wereley, "Variable Recruitment Testing of Pneumatic Artificial Muscles for Robotic Manipulators," *IEEE/ASME Transactions on Mechatronics*, vol. 20, no. 4, pp. 1642–1652, Aug. 2015, doi: 10.1109/TMECH.2014.2341660.

[7] T. Hassan, M. Cianchetti, M. Moatamedi, B. Mazzolai, C. Laschi, and P. Dario, "Finite-Element Modeling and Design of a Pneumatic Braided Muscle Actuator With Multifunctional Capabilities," *IEEE/ASME Transactions on Mechatronics*, vol. 24, no. 1, pp. 109–119, Feb. 2019, doi: 10.1109/TMECH.2018.2877125.

[8] G. Andrikopoulos, G. Nikolakopoulos, and S. Manesis, "A Survey on applications of Pneumatic Artificial Muscles," in *2011 19th Mediterranean Conference on Control & Automation (MED)*, pp. 1439–1446, Jun. 2011, doi: 10.1109/MED.2011.5982983.

[9] M. E. Sadiq, A. J. Humaidi, S. K. Kadhim, A. Sh. Mahdi, A. Alkhayyat, and I. K. Ibraheem, "Comparative Study of Optimal Nonlinear Control Schemes for Hanging Mass Actuated by Uncertain Pneumatic Muscle," in *2021 IEEE 11th International Conference on System Engineering and Technology (ICSET)*, pp. 78–83, Nov. 2021, doi: 10.1109/ICSET53708.2021.9612530.

[10] M. E. Sadiq, A. J. Humaidi, S. K. Kadhim, A. al Mhdawi, A. Alkhayyat, and I. K. Ibraheem, "Optimal Sliding Mode Control of Single Arm PAM-Actuated Manipulator," in *2021 IEEE 11th International Conference on System Engineering and Technology (ICSET)*, pp. 84–89, 2021, doi: 10.1109/ICSET53708.2021.9612539.

[11] X. Shen, "Nonlinear model-based control of pneumatic artificial muscle servo systems," *Control Eng Pract*, vol. 18, no. 3, pp. 311–317, 2010, doi: https://doi.org/10.1016/j.conengprac.2009.11.010.

[12] T. Choi, J. Lee, and J. Lee, "Control of Artificial Pneumatic Muscle for Robot Application," in *2006 IEEE/RSJ International Conference on Intelligent Robots and Systems*, Oct. 2006, pp. 4896–4901, doi: 10.1109/IROS.2006.282447.

[13] D. X. Ba and K. K. Ahn, "A robust time-delay nonlinear controller for a pneumatic artificial muscle," *International Journal of Precision Engineering and Manufacturing*, vol. 19, no. 1, pp. 23–30, Jan. 2018, doi: 10.1007/s12541-018-0003-5.

[14] Ž. Šitum, P. Trslić, D. Trivić, V. Štahan, H. Brezak, and D. Sremić, "Pneumatic muscle actuators within robotic and mechatronic systems," in *Proceedings of International Conference Fluid Power, Fluidna tehnika 2015*, 2015, pp. 175–188.

[15] T. Karnjanaparichat and R. Pongvuthithum, "Adaptive control for a one-link robot arm actuated by pneumatic muscles," *Chiang Mai J. Sci*, vol. 35, no. 3, pp. 437–446, 2008.

[16] J. H. Lilly, "Adaptive tracking for pneumatic muscle actuators in bicep and tricep configurations," *IEEE Transactions on Neural Systems and Rehabilitation Engineering*, vol. 11, no. 3, pp. 333–339, Sep. 2003, doi: 10.1109/TNSRE.2003.816870.

[17] W. Scaff, O. Horikawa, and M. de S. Guerra Tsuzuki, "Pneumatic Artificial Muscle Optimal Control with Simulated Annealing," *IFAC-PapersOnLine*, vol. 51, no. 27, pp. 333–338, 2018, doi: 10.1016/j.ifacol.2018.11.618.

[18] A. E. A. Enzevaee, M. M. M. Mailah, and S. K. S. Kazi, "Control of a Single Link Robot Arm Actuated by Pneumatic Artificial Muscles Employing Active Force Control and Fuzzy Logic via Hardware-In-the-Loop-Simulation," *Jurnal Mekanikal*, vol. 36, no. 2, 2013.

[19] A. Al-Jodah and L. Khames, "Second order sliding mode controller design for pneumatic artificial muscle," *Journal of Engineering*, vol. 24, no. 1, pp. 159–172, 2018.

[20] G. A. Medrano-Cerda, C. J. Bowler, and D. G. Caldwell, "Adaptive position control of antagonistic pneumatic muscle actuators," in *Proceedings 1995 IEEE/RSJ International Conference on Intelligent Robots and Systems. Human Robot Interaction and Cooperative Robots*, vol. 1, pp. 378–383, 1995, doi: 10.1109/IROS.1995.525824.

[21] S. Boudoua, M. Hamerlain, and F. Hamerlain, "Intelligent twisting sliding mode controller using neural network for pneumatic artificial muscles robot arm," in *2015 International Workshop on Recent Advances in Sliding Modes (RASM)*, pp. 1–6, 2015, doi: 10.1109/RASM.2015.7154592.

[22] H. Jahanabadi, M. Mailah, M. Z. Md Zain, and H. M. Hooi, "Active force with fuzzy logic control of a two-link arm driven by pneumatic artificial muscles," *J Bionic Eng*, vol. 8, no. 4, pp. 474–484, Dec. 2011, doi: 10.1016/S1672-6529(11)60053-X.

[23] X. S. Yang, "Bat algorithm for multi-objective optimisation," *International Journal of Bio-Inspired Computation*, vol. 3, no. 5, p. 267, 2011, doi: 10.1504/IJBIC.2011.042259.

[24] "Users guide of FESTO Company." https://www.festo.com/us/en/c/products/industrial-automation/actuators-and-drives/pneumatic-cylinders/diaphragm-actuators/pneumatic-muscle-id_pim397/ (accessed Aug. 12, 2022).

[25] J. H. Lilly and Liang Yang, "Sliding mode tracking for pneumatic muscle actuators in opposing pair configuration," *IEEE Transactions on Control Systems Technology*, vol. 13, no. 4, pp. 550–558, Jul. 2005, doi: 10.1109/TCST.2005.847333.

[26] L. Yang and J. H. Lilly, "Sliding mode tracking for pneumatic muscle actuators in bicep/tricep pair configuration," in *Proceedings of the 2003 American Control Conference, 2003.*, 2003, vol. 6, pp. 4669–4674 vol.6. doi: 10.1109/ACC.2003.1242460.

[27] A. J. Humaidi, S. K. Kadhim, and A. S. Gataa, "Optimal Adaptive Magnetic Suspension Control of Rotary Impeller for Artificial Heart Pump," *Cybern Syst*, vol. 53, no. 1, pp. 141–167, Jan. 2022, doi: 10.1080/01969722.2021.2008686.

[28] S. Yi, K. Watanabe, and I. Nagai, "Backstepping-based Super-Twisting Sliding Mode Control for a Quadrotor Manipulator with Tiltable Rotors," *Journal of Robotics and Control (JRC)*, vol. 3, no. 2, pp. 128–137, 2022, doi: 10.18196/jrc.v3i2.13368.

[29] S. A. AL-Samarraie and Y. K. Abbas, "Design of a nonlinear speed controller for a dc motor system with unknown external torque based on backstepping approach," *Iraqi journal of computers, communications and control & systems engineering*, vol. 12, no. 1, pp. 1–19, 2012.

[30] A. J. Humaidi, S. K. Kadhim, and A. S. Gataa, "Development of a Novel Optimal Backstepping Control Algorithm of Magnetic Impeller-Bearing System for Artificial Heart Ventricle Pump," *Cybern Syst*, vol. 51, no. 4, pp. 521–541, May 2020, doi: 10.1080/01969722.2020.1758467.

[31] A. Ma'arif, M. Antonio Márquez Vera, M. Sadek Mahmoud, S. Ladaci, A. Çakan, and J. Niño Parada, "Backstepping Sliding Mode Control for Inverted Pendulum System with Disturbance and Parameter Uncertainty," *Journal of Robotics and Control (JRC)*, vol. 3, no. 1, pp. 86–92, Nov. 2021, doi: 10.18196/jrc.v3i1.12739.

[32] M. A. Salman and S. K. Kadhim, "Optimal Backstepping Controller Design for Prosthetic Knee Joint," *Journal Européen des Systèmes Automatisés*, vol. 55, no. 1, pp. 49–59, 2022, doi: https://doi.org/10.18280/jesa.550105.

[33] M. Y. Hassan, A. J. Humaidi, and M. K. Hamza, "On the design of backstepping controller for Acrobot system based on adaptive observer," *International Review of Electrical Engineering (IREE)*, vol. 15, no. 4, pp. 328–335, 2020.

[34] A. J. Humaidi and M. R. Hameed, "Design and performance investigation of block-backstepping algorithms for ball and arc system," in *2017 IEEE International Conference on Power, Control, Signals and Instrumentation Engineering (ICPCSI)*, pp. 325–332, 2017, doi: 10.1109/ICPCSI.2017.8392309.

[35] A. Ma'arif, M. A. M. Vera, M. S. Mahmoud, S. Ladaci, A. Çakan, and J. N. Parada, "Backstepping sliding mode control for inverted pendulum system with disturbance and parameter uncertainty," *Journal of Robotics and Control (JRC)*, vol. 3, no. 1, pp. 86–92, 2022, doi: 10.18196/jrc.v3i1.12739.

[36] A. J. Humaidi, M. R. Hameed, and A. H. Hameed, "Design of block-backstepping controller to ball and arc system based on zero dynamic theory," *Journal of Engineering Science and Technology*, vol. 13, no. 7, pp. 2084–2105, 2018.

[37] E. S. Rahayu, A. Ma'arif, and A. Çakan, "Particle Swarm Optimization (PSO) Tuning of PID Control on DC Motor," *International Journal of Robotics and Control Systems*, vol. 2, no. 2, pp. 435–447, 2022, doi: https://doi.org/10.31763/ijrcs.v2i2.476.

[38] O. Muhammed Neda and A. Ma'arif, "Chaotic Particle Swarm Optimization for Solving Reactive Power Optimization Problem," *International Journal of Robotics and Control Systems*, vol. 1, no. 4, pp. 523–533, Jan. 2022, doi: 10.31763/ijrcs.v1i4.539.
[39] B. AlKhlidi, A. T. Abdulsadda, and A. al Bakri, "Optimal Robotic Path Planning Using Intelligents Search Algorithms," *Journal of Robotics and Control (JRC)*, vol. 2, no. 6, pp. 519–526, 2021, doi: 10.18196/jrc.26132.
[40] A. K. Kashyap, D. Parhi, and A. Pandey, "Improved modified chaotic invasive weed optimization approach to solve multi-target assignment for humanoid robot," *Journal of Robotics and Control (JRC)*, vol. 2, no. 3, pp. 194–199, 2021, doi: 10.18196/jrc.2377.
[41] G. Wu, C. Cui, and G. Wu, "Dynamic Modeling and Torque Feedforward based Optimal Fuzzy PD control of a High-Speed Parallel Manipulator," *Journal of Robotics and Control (JRC)*, vol. 2, no. 6, pp. 527–538, 2021, doi: 10.18196/jrc.26133.
[42] X.-S. Yang, "A New Metaheuristic Bat-Inspired Algorithm," in *Nature inspired cooperative strategies for optimization (NICSO 2010)*, Springer, pp. 65–74, 2010, doi: 10.1007/978-3-642-12538-6_6.
[43] K. Hussin, A. Nahar, and H. Khleaf, "A Visual Enhancement Quality of Digital Medical Image Based on Bat Optimization," *Engineering and Technology Journal*, vol. 39, no. 10, pp. 1550–1570, Oct. 2021, doi: 10.30684/etj.v39i10.2165.
[44] M. Rahmani, A. Ghanbari, and M. M. Ettefagh, "Robust adaptive control of a bio-inspired robot manipulator using bat algorithm," *Expert Syst Appl*, vol. 56, pp. 164–176, Sep. 2016, doi: 10.1016/j.eswa.2016.03.006.
[45] L. Rasheed, "A Comparative Study of Various Intelligent Controllers' Performance for Systems Based on Bat Optimization Algorithm," *Engineering and Technology Journal*, vol. 38, no. 6, pp. 938–950, Jun. 2020, doi: 10.30684/etj.v38i6A.622.
[46] A. J. Humaidi, I. K. Ibraheem, A. T. Azar, and M. E. Sadiq, "A New Adaptive Synergetic Control Design for Single Link Robot Arm Actuated by Pneumatic Muscles," *Entropy*, vol. 22, no. 7, p. 723, Jun. 2020, doi: 10.3390/e22070723.